# Dynamics of Active Filaments in Porous Media

Zahra Mokhtari and Annette Zippelius
*Institute for Theoretical Physics, Friedrich-Hund-Platz 1, 37077 Göttingen, Germany*

(Received 8 March 2019; published 9 July 2019)

The motion of active polymers in a two-dimensional porous medium is shown to depend critically on flexibility, activity, and degree of polymerization. For a given Péclet number, we observe a transition from localization to diffusion as the stiffness of the chains is increased. Whereas stiff chains move almost unhindered through the porous medium, flexible ones spiral and get stuck. Their motion can be accounted for by the model of a continuous time random walk with a renewal process corresponding to unspiraling. The waiting time distribution is shown to develop heavy tails for decreasing stiffness, resulting in subdiffusive and ultimately caged behavior.

DOI: 10.1103/PhysRevLett.123.028001

Understanding the motion of biological agents in porous media is essential for a wide range of biological, medical, and industrial processes. Mucus, a hydrogel which coats the stomach and other intestinal walls, serves as an important defense against invading bacteria [1–4]. In fighting cancer, bacteria are now engineered to sense the porous environment of a tumor [5,6]. Other bacteria such as myxobacteria glide in the porous environment of soil and synthesize a number of biomedically useful chemicals [7]. Yet another example of active motion in a porous medium is the crowded world of a cell, in which active filaments move in a polymeric gel. Technical applications involve the motion of bacteria in porous media in the context of oil recovery [8], water purification, and decomposition of contaminants trapped in the ground [9,10].

It is known that the dynamics of biological agents in porous media is strongly influenced by their shape, size, and properties of the media such as the pore sizes [11–13]. In spite of many experimental studies on the motion of active elongated agents in porous media [14–21], theoretical approaches are sparse [22–24]. In contrast, the flow of passive polymers in porous media has been studied extensively. Whereas flexible chains can be represented by a sequence of blobs [25] whose size is determined by the cavities of the porous media, the dynamics of stiff polymers was found to follow the reptation picture [26] with, however, different kinetic exponents.

Bacteria and many other microorganism have an elongated shape and resist deformations with a finite stiffness. Their flexibility plays an important role in their dynamics: While stiff active filaments such as microtubules form large coherently moving bundles [27–29], active agents with flexible bodies, such as bacteria, have been found to form slowly diffusing spirals [30]. Analytical and numerical studies of active filaments have revealed that bundles and spirals form in different regions of phase space, solely determined by the activity and stiffness of the chains [31–33]. Flexibility is even more important in a crowded environment: a large number of biological agents maximize their transport by deforming their shape depending on the environment and interaction with other objects [34,35]. The interest in active elongated agents is further driven by new developments to prepare them *in vitro* [36–38] and synthesize them, e.g., by means of bonding several Janus colloidal spheres through electric fields [39], and also by immersing chains of passive colloidal particles in an active bath, where directed transport has been observed [40].

In this work we analyze the motion of self-propelled filaments in a two-dimensional porous medium with the help of numerical simulations, supported by analytical arguments. Our main result is a phase diagram with a diffusive and a localized phase, whose intuitive interpretation is based on the competition between the activity driving the polymers through narrow channels and the flexibility favoring a spiraling, or more generally, folded, state of the filaments which then are caged in the porous medium.

Our model consists of three parts: a standard model for a semiflexible chain, overdamped dynamics of the chain including active beads, and an ensemble of static obstacles. We consider a wormlike chain, consisting of $M$ active beads of radius $R$ at positions $r_i$, $i = 1, 2, \ldots, M$. The potential energy $U_{\mathrm{pol}} = U_s + U_b + U_e$ of the chain has three contributions. The connectivity of the chain is modeled by springs with spring constant $K_s$ and rest length $b$. The bending energy is given by

$$U_b = \frac{K_a}{2}\sum_{i=2}^{M-1}(\theta_i - \pi)^2, \qquad \cos\theta_i = \frac{\mathbf{r}_{i,i-1}\cdot\mathbf{r}_{i+1,i}}{r_{i,i-1}r_{i+1,i}}, \quad (1)$$

with $\mathbf{r}_{i,i-1} = \mathbf{r}_i - \mathbf{r}_{i-1}$ and bending stiffness $K_a$. The excluded volume is modeled as a contact potential:

 

$$U_e = \frac{1}{2} K_e \sum_{i \neq j} (r_{i,j} - 2R)^2 \theta(2R - r_{i,j}). \tag{2}$$

We are interested in approximately hard particles of fixed bond length and hence take both $K_s$ and $K_e$ to be large. To avoid chain crossings, the bond length $b = 2.1R$ is chosen only slightly larger than the diameter of the beads. This leaves us with one free parameter, namely the bond stiffness $K_a$, or rather the persistence length $\xi/L = 2bK_a/(LK_BT)$ relative to the contour length $L = Mb$.

The dynamics of the chain is assumed to be overdamped,

$$\gamma \dot{\mathbf{r}}_i = F_{\text{act}} \mathbf{t}_i - \nabla_i U + \boldsymbol{\eta}_i. \tag{3}$$

The active force has amplitude $F_{\text{act}}$ and points along the tangent of the polymer contour, $\mathbf{t}_i = (\mathbf{r}_{i,i-1} + \mathbf{r}_{i+1,i})/|\mathbf{r}_{i,i-1} + \mathbf{r}_{i+1,i}|$. The potential $U$ includes $U_{\text{pol}}$ as well as the interactions with the obstacles, yet to be specified. The damping constant is denoted by $\gamma$ and the random noise is chosen in accordance with the fluctuation dissipation theorem: $\langle \boldsymbol{\eta}_i(t) \cdot \boldsymbol{\eta}_j(t') \rangle = 4k_BT\delta_{ij}\gamma\delta(t - t')$. It is convenient to work with dimensionless equations. Hence we measure length in units of particle radius $R$, energies in units of $k_BT$, and time in units of $t_0 = R^2\gamma/(k_BT)$. In these units the active force is given by $(F_{\text{act}}R)/(k_BT)$ and represents the second control parameter besides the persistence length. Actually, it is more convenient to multiply this quantity by the dimensionless factor $L^2/(bR)$ in order to obtain the Péclet number $\text{Pe} = (F_{\text{act}}L^2)/(bk_BT)$, which is defined as the ratio of the convective transport to the diffusive transport.

So far our model is the same as the one used in Ref. [32]. However, here we are interested in the dynamics of semiflexible chains in a crowded environment. We introduce $N$ static obstacles of radius $R_o$ randomly into a two-dimensional square box of size $\ell$. The interactions between particles and obstacles are modeled as elastic collisions, reversing the normal component of the relative velocity [41]. We impose the constraint that obstacles do not overlap, so that their packing fraction is given by $\phi = N\pi R_o^2/\ell^2$. Of particular interest is a porous medium with a typical pore size, which is modeled with the help of an additional constraint: the relative distance between any two obstacles is at least $2R_o + 2.5R$, allowing single beads to pass in between two obstacles. The central questions of our study are the following. Are the polymers free to move through the medium or are they localized? How does their dynamics depend on chain length, stiffness, and Péclet number? A similar porous medium has been set up in a recent experiment [15], where the motion of bacteria in the presence of randomly placed pillars in microfluidic chips has been studied.

Equation (3) was integrated using HOOMD-BLUE [42,43] with an in-house modification to include the active force along the tangent of the polymer contour. Simulations were performed on graphical processing units. We set $K_s = K_e = 500k_BT/R^2$ and $M = 30$ unless stated otherwise, and explore a large parameter space for Pe and $\xi/L$ by varying $F_{\text{act}}$ and $K_a$. Measurements are carried out after an initial time lapse, and for as long as $10^6 t_0$.

The central topic of our Letter is the selective localization of stiff and flexible polymers in an obstructed medium. Before addressing this subject in detail, we comment on the diffusion of semiflexible polymers in an unobstructed environment which has been discussed in recent literature [32,33,44]. One of the most prominent results is the spiraling phase, where flexible polymers form persistent spirals. We of course also observe these states, sometimes the flexible polymers spiral around an obstacle, provided their contour length is larger than the circumference of the obstacle. These results are to be expected and a sample configuration is shown in Fig. 1. The stiff polymers tend to follow the obstacles only for short sections of their contour length, compromising the cost of bending energy and activity $F_{\text{act}}L$. This qualitatively different behaviour is at the heart of the selective transport, discussed in detail below.

For a single polymer, obeying the dynamics of Eq. (3), we can compute the center of mass diffusion (without obstacles) because all interactions are pairwise and do not contribute to the c.m. motion:

$$\dot{\mathbf{R}}_{\text{c.m.}} = \frac{F_{\text{act}}}{\gamma L} \mathbf{R}_e + \frac{1}{M} \sum_{i=1}^{M} \boldsymbol{\eta}_i. \tag{4}$$

Here $\mathbf{R}_e$ denotes the end-to-end vector. Since the activity points along the contour, the polymer motion is well approximated by "railway motion" [32], allowing for the computation of the end-to-end vector within the Kratky-Porod model. The mean square displacement (MSD) then follows

$$\langle (\mathbf{R}(t) - \mathbf{R}(0))^2 \rangle = 4D_t t + \frac{2\xi F_{\text{act}}}{\gamma} f(L/\xi)[t + (e^{-D_r t} - 1)/D_r]. \tag{5}$$

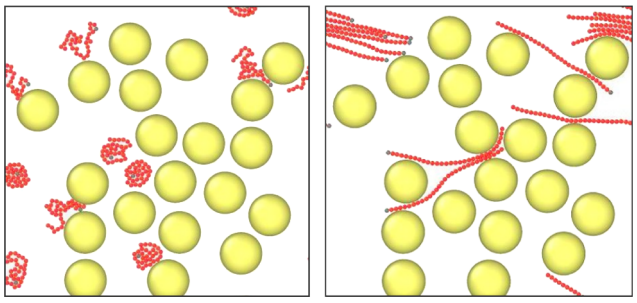

FIG. 1. Flexible polymers (left) spiral, sometimes around the obstacles; stiff polymers (right) bend only slightly to pass around an obstacle.

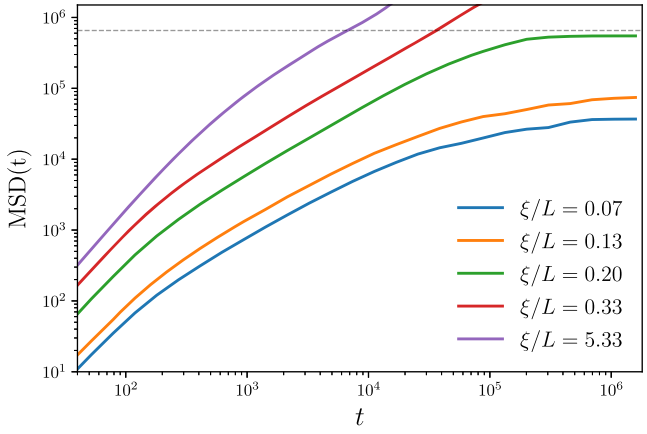


FIG. 2. Mean square displacement of active chains for Pe = 945 and different values of stiffness: from $\xi/L = 0.07$ ($K_a = 1$) to $\xi/L = 5.33$ ($K_a = 80$) at $\phi = 0.6$. The black line indicates the system size.

The activity induced rotational diffusion constant is given by $D_r = F_{\rm act}/(\xi\gamma)$ [32] and $f(x) = 2(e^{-x} - 1 + x)/x^2$. The dynamics is diffusive for short times with bare diffusion constant $D_t = (k_B T)/(\gamma M)$, ballistic for intermediate times, and diffusive again at long times with, however, an enhanced diffusion constant $D_{\rm eff} = D_t + F_{\rm act}\xi f(L/\xi)/(2\gamma)$, due to the activity of the chain.

Our focus here is on the dynamics of active polymers in a porous medium. As a first step we have computed the MSD for various values of the parameters for filling fraction $\phi = 0.6$. An example is shown in Fig. 2 for $M = 30$ and varying stiffness. For $\xi/L < 0.2$, we observe three different regimes: ballistic due to activity at small $t$, diffusive at intermediate $t$, and saturated or caged for the largest $t$. For larger $\xi/L$, the polymers are seen to move through the whole sample; for $\xi/L = 0.33$, one can still observe the crossover from ballistic to diffusive motion, whereas for very large $\xi/L$ the motion is ballistic almost up to system size. Some trajectories of the very stiff polymers are depicted in the left-hand panel of Fig. 3 [see also Supplemental Material (SM) [45]].

If not all flexible polymers are localized, then the mobile ones will dominate the MSD for long times. Hence we need a better indicator for localization, e.g., the fraction of polymers which have moved less than a given distance $d$, comparable to the system size. We define $Q(t) = \langle\theta(d - |\mathbf{R}(t_0 + t) - \mathbf{R}(t_0)|)\rangle$, where the average is over many different polymers. We show $Q(t)$ for $d = \ell/8$ in Fig. 4 for the same data as in Fig. 2. One clearly observes a time-persistent part for the smallest values of $\xi/L$, indicating that a finite fraction of the polymers is localized in good agreement with the data from the MSD. Furthermore, the relaxation time of $Q(t)$ grows with decreasing $\xi/L$ and diverges at the critical $\xi$. The inset in Fig. 4 displays the time $\tau_Q$, when more than 20% of the particles have moved by more than $d$.

Flexible polymers are localized in the porous medium because they tend to spiral or fold into a dense state which does not allow them to pass through the narrow channels. To quantify this statement, we have computed the radius of gyration for the above set of parameters, i.e., $\phi = 0.6$ and $M = 30$. The result is plotted in the inset of Fig. 5; a clear transition is observed from the dense to the extended state at around $\xi/L = 0.2$. To pass through the narrow channels, the polymers have to unspiral, which is a rare event, even in a system without obstacles and more so in the presence of obstacles. This can be demonstrated by monitoring the fraction of polymers which have not unspiraled once in time $t$. We denote this fraction by $Y(t)$ and plot it for various values of the stiffness in Fig. 5. One clearly observes a time-persistent part for $\xi/L \leq 0.2$.

How do these results depend on Péclet number? Spiraling of flexible polymers is enhanced by high activity or high Péclet number, as evidenced by the strong spiraling regime in Ref. [32]. Hence, increasing the Péclet number implies a stronger tendency to localization, as displayed in the phase diagram shown in Fig. 6: even stiffer chains get localized with increasing Pe. On the other hand, high activity favors directed motion in the extended state. For Pe $\geq 3000$, we observe an increased fraction of time in the extended state and hence also an increase in the size of the

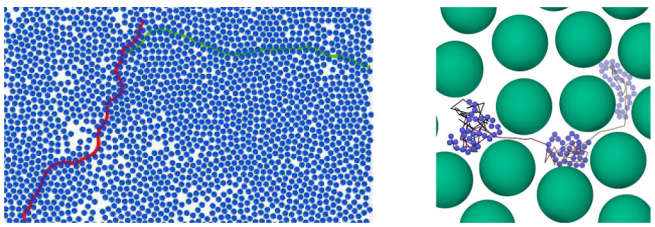

FIG. 3. Trajectory $\mathbf{R}_{\rm c.m.}(t)$ of stiff filaments ($\xi_p/L = 30$) for a time span $\tau \approx 2000$ (left). Trajectory of a flexible filament, which curls up and rarely jumps to nearby sites (right).

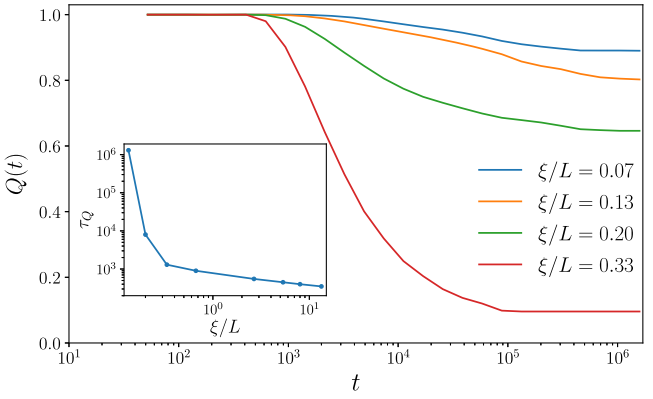


FIG. 4. Fraction of polymers $Q(t)$ which have moved less than $d = \ell/8$ in time $t$ for several values of persistence length. Inset: Relaxation time $\tau_Q$, when $Q(t)$ has decayed to 20% of its initial value.

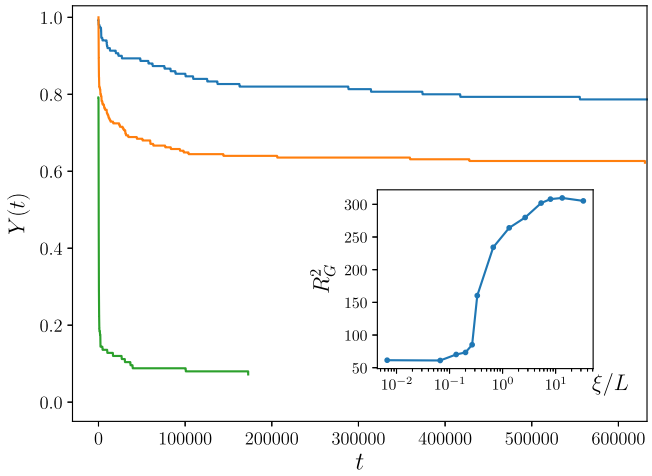


FIG. 5. Fraction of polymers which have not at least unspiraled once in time $t$. Parameters are $\xi/L = 0.07, 0.20, 0.33$ from top to bottom, $\phi = 0.6$, $M = 30$. Inset: Radius of gyration as a function of $\xi/L$; fully extended state corresponds to $R_G \sim 330$.

random steps taken in the extended state, giving rise to diffusion for the largest Pe (see SM [45]). Localization also depends on the degree of polymerization $M$. Whereas the dynamics of the very stiff filaments is hardly affected, spiraling and hence localization can only occur for sufficiently long chains (see SM [45]).

Flexible polymers have to unwind before they can move through the narrow channels of the obstructed environment. Our simulations show that a flexible chain is most of the time in a dense state, unspirals infrequently, makes a sudden jump in the extended state, and immediately curls up again (see right-hand panel of Fig. 3 and SM [45]). In a simple model, we neglect the time span in the stretched state so that the dynamics can be modeled by instantaneous jumps of typical size $\Delta R$, separated by random time intervals $\tau$. The unspiraling of the flexible polymers then corresponds to the renewal process of a continuous time random walk (CTRW) [46]. The "renewals" are the unspiraling events, allowing the polymer to make a displacement. The central quantity is the distribution of waiting times $\psi(\tau)$, where $\tau$ denotes the difference between two unspiraling events.The mean square displacement,

$$\langle (\mathbf{R}(t) - \mathbf{R}(0))^2 \rangle = \langle n(t) \rangle \Delta R^2, \tag{6}$$

is expressed in terms of $\langle n(t) \rangle$, the mean number of jumps in time $t$. It can be calculated from $\psi(\tau)$:

$$\langle n(s) \rangle = \frac{\psi(s)}{s[1 - \psi(s)]}. \tag{7}$$

Here we have introduced the Laplace transform of $n(s) = \int_0^t dt n(t) e^{-st}$ and similarly for $\psi(s)$. The low frequency behavior of $\psi(s)$ determines the longtime behavior of $\langle n(t) \rangle$ and hence the MSD. If $\psi(s) \sim 1 - s\langle \tau \rangle$ is regular for samll $s$, then the MSD displays ordinary diffusion. If, on the other hand, $\psi(s) \sim 1 - As^\alpha$ with $\alpha < 1$, then the MSD is given by [47]

$$\langle (\mathbf{R}(t) - \mathbf{R}(0))^2 \rangle = \frac{\Delta R^2}{A\Gamma(1+\alpha)} t^\alpha. \tag{8}$$

Hence, subdiffusive behavior should occur and saturation for $\alpha = 0$. We have measured $\psi(\tau)$ for several values of stiffness $K_a$. An example is shown in Fig. 7. One clearly observes a heavy tail with an algebraic decay approximately like $t^{-1.3}$, which implies subdiffusive behavior $\langle (\mathbf{R}(t) - \mathbf{R}(0))^2 \rangle \sim t^{0.3}$ for the MSD. Because of limited simulation time, we are missing the very long times, which would lower the exponent to even smaller values. In the inset of Fig. 7, we compare the MSD from our simulations to the result of CTRW as given in Eq. (6).

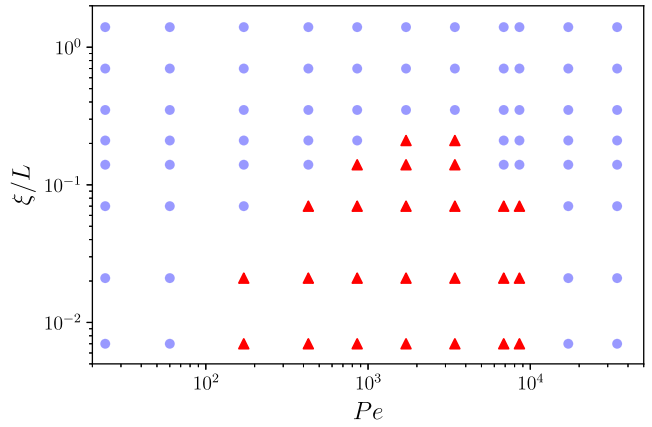


FIG. 6. Phase diagram in the $\xi/L$ and Pe plane. Parameters are $\phi = 0.6$ and $M = 30$. Triangles, localized phase; circle, diffusive regime.

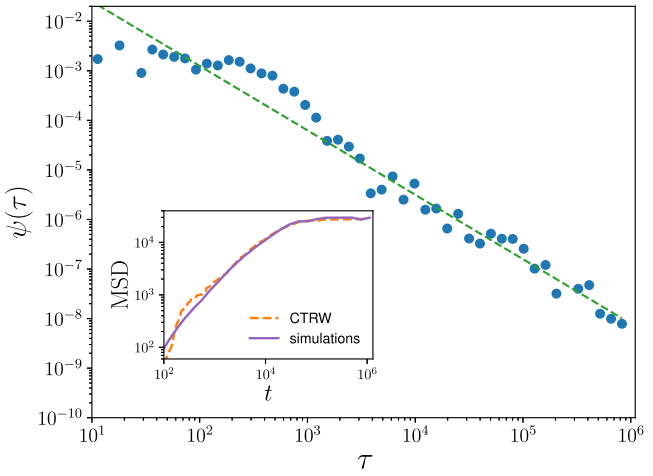


FIG. 7. Waiting time distribution $\psi(\tau)$ for $\xi/L = 0.07$ and Pe $= 945$. Inset: Comparison of MSD computed from Eq. (6) with simulations.

In conclusion, active polymers in porous media show unexpected, rich behavior. Whereas stiff chains are able to cross the porous medium from one side to the other, flexible chains spiral and are caged. Thus, a localization transition occurs as a function of chain stiffness and Péclet number. We have worked out the phase in the $\xi/L - \mathrm{Pe}$ plane and estimated the effects of chain length. Localization of flexible chains occurs due to the persistence of the spiraling state. Identifying unspiraling as a renewal event, we can model the dynamics of flexible chains as a continuous time random walk. The distribution of waiting times between the renewal events was shown to develop a heavy tail, as the localization transition is approached, giving rise to subdiffusive behavior and ultimately caging.

Many extensions of our work lie ahead: Porous media exist in a variety of geometries and topologies, giving rise to correspondingly diverse dynamics of active polymers. An example is the interplay of pore size, filling fraction, and chain length in a dense gel. Another possible extension are more general models of a crowded environment, which is not strictly static but moving slowly as compared to the active agent (see Supplemental Material [45]). Other mechanisms of activity are also of interest, such as a dragged chain or the inclusion of a tumbling component [48].


[1] S. Cornick, A. Tawiah, and K. Chadee, Roles and regulation of the mucus barrier in the gut, Tissue Barriers **3**, e982426 (2015).

[2] D. C. Laux, P. S. Cohen, and T. Conway, Role of the mucus layer in bacterial colonization of the intestine, in *Colonization of Mucosal Surfaces* (American Society of Microbiology, 2005), pp. 199–212.

[3] P. S. Cohen and D. C. Laux, Bacterial adhesion to and penetration of intestinal mucus in vitro, in *Methods in Enzymology* (Elsevier, New York, 1995), Vol. 253, pp. 309–314.

[4] J. P. Celli, B. S. Turner, N. H. Afdhal, S. Keates, I. Ghiran, C. P. Kelly, R. H. Ewoldt, G. H. McKinley, P. So, S. Erramilli *et al.*, Helicobacter pylori moves through mucus by reducing mucin viscoelasticity, Proc. Natl. Acad. Sci. U.S.A. **106**, 14321 (2009).

[5] J. C. Anderson, E. J. Clarke, A. P. Arkin, and C. A. Voigt, Environmentally controlled invasion of cancer cells by engineered bacteria, J. Mol. Biol. **355**, 619 (2006).

[6] O. Felfoul, M. Mohammadi, S. Taherkhani, D. De Lanauze, Y. Z. Xu, D. Loghin, S. Essa, S. Jancik, D. Houle, M. Lafleur *et al.*, Magneto-aerotactic bacteria deliver drug-containing nanoliposomes to tumour hypoxic regions, Nat. Nanotechnol. **11**, 941 (2016).

[7] W. Dawid, Biology and global distribution of myxobacteria in soils, FEMS Microbiol. Rev. **24**, 403 (2000).

[8] L. R. Brown, Microbial enhanced oil recovery (meor), Curr. Opin. Microbiol. **13**, 316 (2010).

[9] T. R. Ginn, B. D. Wood, K. E. Nelson, T. D. Scheibe, E. M. Murphy, and T. Prabhakar Clement, Processes in microbial transport in the natural subsurface, Adv. Water Resour. **25**, 1017 (2002).

[10] F.-G. Simon, T. Meggyes, and T. Tünnermeier, Groundwater remediation using active and passive processes, *Advanced Groundwater Remediation: Active and Passive Technologies* (Thomas Telford Publishing, London, 2002), pp. 3–29.

[11] S. E. Spagnolie, B. Liu, and T. R. Powers, Locomotion of Helical Bodies in Viscoelastic Fluids: Enhanced Swimming at Large Helical Amplitudes, Phys. Rev. Lett. **111**, 068101 (2013).

[12] H. C. Fu, V. B. Shenoy, and T. R. Powers, Low-Reynolds-number swimming in gels, Europhys. Lett. **91**, 24002 (2010).

[13] A. M. Leshansky, Enhanced low-Reynolds-number propulsion in heterogeneous viscous environments, Phys. Rev. E **80**, 051911 (2009).

[14] O. A. Croze, G. P. Ferguson, M. E. Cates, and W. C. K. Poon, Migration of chemotactic bacteria in soft agar: Role of gel concentration, Biophys. J. **101**, 525 (2011).

[15] A. Creppy, E. Clément, C. Douarche, M. Veronica D'Angelo, and H. Auradou, Effect of motility on the transport of bacteria populations through a porous medium, Phys. Rev. Fluids **4**, 013102 (2019).

[16] A. T. Brown, I. D. Vladescu, A. Dawson, T. Vissers, J. Schwarz-Linek, J. S. Lintuvuori, and W. C. K. Poon, Swimming in a crystal, Soft Matter **12**, 131 (2016).

[17] A. J. Wolfe and H. C. Berg, Migration of bacteria in semisolid agar, Proc. Natl. Acad. Sci. U.S.A. **86**, 6973 (1989).

[18] V. A. Martinez, J. Schwarz-Linek, M. Reufer, L. G. Wilson, A. N. Morozov, and W. C. K. Poon, Flagellated bacterial motility in polymer solutions, Proc. Natl. Acad. Sci. U.S.A. **111**, 17771 (2014).

[19] J. E. Sosa-Hernández, M. Santillán, and J. Santana-Solano, Motility of Escherichia coli in a quasi-two-dimensional porous medium, Phys. Rev. E **95**, 032404 (2017).

[20] M. Raatz, M. Hintsche, M. Bahrs, M. Theves, and C. Beta, Swimming patterns of a polarly flagellated bacterium in environments of increasing complexity, Eur. Phys. J. Spec. Top. **224**, 1185 (2015).

[21] T. Bhattacharjee and S. S. Datta, Bacterial hopping and trapping in porous media, Nat. Commun. **10**, 2075 (2019).

[22] J. W. Barton and R. M. Ford, Mathematical model for characterization of bacterial migration through sand cores, Biotechnol. Bioeng. **53**, 487 (1997).

[23] T. Bertrand, Y. Zhao, O. Bénichou, J. Tailleur, and R. Voituriez, Optimized Diffusion of Run-and-Tumble Particles in Crowded Environments, Phys. Rev. Lett. **120**, 198103 (2018).

[24] O. Chepizhko and F. Peruani, Diffusion, Subdiffusion, and Trapping of Active Particles in Heterogeneous Media, Phys. Rev. Lett. **111**, 160604 (2013).

[25] V. Yamakov and A. Milchev, Diffusion of a polymer chain in porous media, Phys. Rev. E **55**, 1704 (1997).

[26] G. Nam, A. Johner, and M.-K. Lee, Reptation of a semiflexible polymer through porous media, J. Chem. Phys. **133**, 044908 (2010).

[27] T. Sanchez, D. Welch, D. Nicastro, and Z. Dogic, Cilia-like beating of active microtubule bundles, Science **333**, 456 (2011).
[28] A. T. Lam, V. VanDelinder, A. M. R. Kabir, H. Hess, G. D. Bachand, and A. Kakugo, Cytoskeletal motor-driven active self-assembly in in vitro systems, Soft Matter **12**, 988 (2016).
[29] D. Inoue, B. Mahmot, A. Md Rashedul Kabir, T. I. Farhana, K. Tokuraku, K. Sada, A. Konagaya, and A. Kakugo, Depletion force induced collective motion of microtubules driven by kinesin, Nanoscale **7**, 18054 (2015).
[30] S.-N. Lin, W.-C. Lo, and C.-J. Lo, Dynamics of self-organized rotating spiral-coils in bacterial swarms, Soft Matter **10**, 760 (2014).
[31] T. B. Liverpool, Anomalous fluctuations of active polar filaments, Phys. Rev. E **67**, 031909 (2003).
[32] R. E. Isele-Holder, J. Elgeti, and G. Gompper, Self-propelled worm-like filaments: Spontaneous spiral formation, structure, and dynamics, Soft Matter **11**, 7181 (2015).
[33] K. R. Prathyusha, S. Henkes, and R. Sknepnek, Dynamically generated patterns in dense suspensions of active filaments, Phys. Rev. E **97**, 022606 (2018).
[34] A. M. Menzel and T. Ohta, Soft deformable self-propelled particles, Europhys. Lett. **99**, 58001 (2012).
[35] T. Ohta and T. Ohkuma, Deformable Self-Propelled Particles, Phys. Rev. Lett. **102**, 154101 (2009).
[36] V. Schaller, C. Weber, C. Semmrich, E. Frey, and A. R. Bausch, Polar patterns of driven filaments, Nature (London) **467**, 73 (2010).
[37] Y. Sumino, K. H Nagai, Y. Shitaka, D. Tanaka, K. Yoshikawa, H. Chaté, and K. Oiwa, Large-scale vortex lattice emerging from collectively moving microtubules, Nature (London) **483**, 448 (2012).
[38] P. Kraikivski, R. Lipowsky, and J. Kierfeld, Enhanced Ordering of Interacting Filaments by Molecular Motors, Phys. Rev. Lett. **96**, 258103 (2006).
[39] J. Yan, M. Han, J. Zhang, C. Xu, E. Luijten, and S. Granick, Reconfiguring active particles by electrostatic imbalance, Nat. Mater. **15**, 1095 (2016).
[40] Y. Sasaki, Y. Takikawa, V. S. R. Jampani, H. Hoshikawa, T. Seto, C. Bahr, S. Herminghaus, Y. Hidaka, and H. Orihara, Colloidal caterpillars for cargo transportation, Soft Matter **10**, 8813 (2014).
[41] Z. Mokhtari, T. Aspelmeier, and A. Zippelius, Collective rotations of active particles interacting with obstacles, Europhys. Lett. **120**, 14001 (2017).
[42] J. A. Anderson, C. D. Lorenz, and A. Travesset, General purpose molecular dynamics simulations fully implemented on graphics processing units, J. Comput. Phys. **227**, 5342 (2008).
[43] J. Glaser, T. D. Nguyen, J. A. Anderson, P. Lui, F. Spiga, J. A. Millan, D. C. Morse, and S. C. Glotzer, Strong scaling of general-purpose molecular dynamics simulations on GPUs, Comput. Phys. Commun. **192**, 97 (2015).
[44] Ö. Duman, R. E. Isele-Holder, J. Elgeti, and G. Gompper, Collective dynamics of self-propelled semi-flexible filaments, Soft Matter **14**, 4483 (2018).
[45] See Supplemental Material at http://link.aps.org/supplemental/10.1103/PhysRevLett.123.028001 for movies and further analysis.
[46] E. W. Montroll and G. H. Weiss, Random walks on lattices. II, J. Math. Phys. (N.Y.) **6**, 167 (1965).
[47] E. Barkai, Stochastic processes in physics 2008, 2010, 2014, https://faculty.biu.ac.il/~barkaie/teaching.html.
[48] N. A. Licata, B. Mohari, C. Fuqua, and S. Setayeshgar, Diffusion of bacterial cells in porous media, Biophys. J. **110**, 247 (2016).